Numerical Analysis of the Photoeffects in GaAs MESFET's

Shih-Hsien Lo, *Student Member, IEEE,* and Chien-Ping Lee, *Member, IEEE*

Abstract—**The photoeffects on the *I–V* characteristics of GaAs MESFET's have been studied by a two-dimensional numerical method. It is theoretically verified that the photovoltaic effect occurring at the channel/substrate interface is responsible for the substantial increase of the drain current. The reverse gate current due to illumination is caused by sweep-out by the high electrical field in the gate depletion region, where a large gradient in the depth profile of the hole Fermi energy is found. For devices with a lightly doped n-type buffer layer, the increase of the drain current is less than for devices without a buffer layer, but is still substantial.**

Nomenclature

- D_n Diffusion coefficient for electrons.
- D_p Diffusion coefficient for holes.
- E Electrical field.
- E_F Hole Fermi energy without illumination.
- E_{F_p} Hole Fermi energy with illumination.
- E_G Energy gap of GaAs.
- E_i Intrinsic Fermi level.
- E_t Cr-related trap energy level.
- G_{opt} Photogeneration rate.
- I_D Drain current.
- I_G Gate current.
- J_n Electron current density.
- J_p Hole current density.
- n Free electron concentration.
- N_D Donor concentration.
- n_i Intrinsic concentration.
- N_{SD}^+ Residual donor concentration in the substrate.
- N_T Cr-related trap concentration in the substrate.
- N_T^- Occupied Cr-related trap concentration in the substrate.
- p Hole concentration.
- q Electron charge.
- R Net recombination rate.
- T Temperature.
- v_s Saturation velocity.
- v_{th} Thermal velocity.
- V_D Drain voltage.
- V_G Gate voltage.
- y Depth from the top free surface of devices.
- α Light absorption coefficient ($\approx 1 \times 10^4$ cm^{-1} for $\lambda = 0.83$–0.87 μm).
- ϵ Permittivity of GaAs.
- λ Wavelength of light.
- μ_0 Low-field mobility.
- μ_n Electron mobility (cm^2/V · s).
- μ_p Hole mobility (cm^2/V · s).
- Φ Photon flux (cm^{-2} · s^{-1}).
- ψ Electrostatic potential.
- σ_n Capture cross section for electrons.
- σ_p Capture cross section for holes.

Manuscript received April 25, 1991; revised December 20, 1991. This work was supported by the National Science Council of the Republic of China. The review of this paper was arranged by Associate Editor N. Moll.

The authors are with the Department of Electronics Engineering and the Institute of Electronics, National Chiao Tung University, Hsinchu, Taiwan, Republic of China.

IEEE Log Number 9200382.

I. Introduction

IN THE LAST DECADE, direct optical control of GaAs MESFET's has received considerable attention for its potential applications in optical communication systems [1]–[9]. For photon energies equal to or greater than the bandgap energy of GaAs (E_G = 1.424 eV at T = 300 K), experimental investigations show that the gain and the drain current of a MESFET can be controlled by incident light intensity in the same manner as varying the gate bias [6], [10]. With such a property, the GaAs MESFET can be used for such functions as a photodetector, optical switching amplifier, or optical/microwave transducer.

Several mechanisms have been suggested to explain the photoeffects in GaAs MESFET's, especially the increase of drain current due to illumination. Graffeuil *et al.* [10] suggested that incident photons cause a change in the built-in voltage of the gate junction and by this mechanism, the drain current increases. Pan [2] suggested that both the photoconductivity effect in the source–gate and the drain–gate regions and the change of the gate depletion width are responsible for the increase of the drain current. Edwards [11] measured a positive voltage across the depletion region between the n-type channel and the semi-insulating substrate and suggested that the drain current increase is closely related to the channel width modulation by the positive voltage. Analytical work has been attempted to understand the photoeffects on the *I–V* characteristics and the device performance of GaAs MESFET's, but these analyses usually assume that the drain current is enhanced either by a photo-induced voltage across the Schottky barrier [7], [12], [13] or by photogenerated carriers below the gate [14], [15].

To shed further light on the mechanisms governing the

photoeffects, both the device structure and the appropriate physical equations governing device behavior should be taken into account. In this work, we have chosen a two-dimensional numerical approach, which makes very few assumptions in solving fundamental device equations and is capable of simulating a realistic device structure for understanding the photoeffects and the underlying mechanism.

II. Simulated Device Structures

In the past, most of the experimental measurements for the photoeffects were made in uniformly doped MESFET's [7], [8]. For this reason, we chose a uniformly doped structure for our study. Two GaAs MESFET structures were simulated in this study. They are shown in Fig. 1(a) and (b). For both structures, the n-type channel is 0.2 μm thick and is uniformly doped with a concentration of 1×10^{17} cm^{-3}. The gate length is 0.5 μm and both the source–gate and the gate–drain spacings are 1.5 μm. For the structure shown in Fig. 1(a), the uniformly doped channel is located directly on the semi-insulating substrate without any buffer layer, while for the other structure as shown in Fig. 1(b), there is a 1 μm, 1×10^{14} cm^{-3}, n-type buffer layer between the n channel and the semi-insulating substrate. The semi-insulating substrate is assumed to be Cr doped with a concentration of 1×10^{16} cm^{-3} [16] and has a residual shallow donor concentration of 1×10^{15} cm^{-3}. For photon energy around the GaAs bandgap energy (1.424 eV), the measured absorption coefficient is about 1×10^{4} cm^{-1} [17]. To encompass the photoeffects and other physical phenomena, the total depth of the simulated device structure is 5 μm.

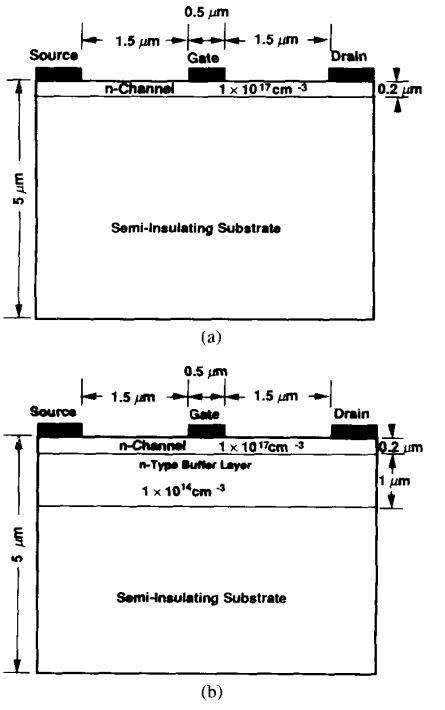

Fig. 1. Device structures (a) without and (b) with an n-type buffer layer in this study.

III. Basic Equations, Boundary Conditions, and Numerical Methods

The basic equations used in this study are as follows:

1) Poisson's equation

$$\nabla^2\psi = -\frac{q}{\epsilon}(p - n + N_D^+ + N_{SD}^+ - N_T^-) \tag{1}$$

where N_{SD}^+ and N_T^- are the concentrations of the residual shallow donor and the occupied Cr-related level, respectively, in the semi-insulating substrate.

2) Drift-diffusion current continuity equations for electrons and holes

$$-\frac{1}{q}\nabla \cdot \boldsymbol{J}_n - G_{\text{opt}} + R = 0 \tag{2}$$

$$\frac{1}{q}\nabla \cdot \boldsymbol{J}_p - G_{\text{opt}} + R = 0. \tag{3}$$

The electron and hole currents are determined from

$$\boldsymbol{J}_n = -q\mu_n n\nabla\psi + qD_n\nabla n \tag{4}$$

$$\boldsymbol{J}_p = -q\mu_p p\nabla\psi - qD_p\nabla p. \tag{5}$$

The net recombination rate R in (2) and (3) includes three kinds of recombination mechanisms: Shockley–Read–Hall (SRH), radiative (i.e., band-to-band), and Auger recombination [18]. In this study, it is assumed that in the channel and in the buffer layer, the intermediate centers assisting in the SRH recombination process are neutral centers located at the intrinsic Fermi level. The lifetimes for holes and electrons are assumed to be 1 ns [19]. In the substrate, the Cr-related traps are deep acceptors. At $T =$ 300 K, the Cr-related deep level is 0.6 eV below the conduction band [20] and the captured cross sections for holes and electrons are assumed to be 1×10^{-14} [16] and 1×10^{-16} cm^2, respectively. In steady state, the occupied trap concentration and the SRH recombination rate in the substrate can be expressed as

$$N_T^- = \frac{\sigma_n n + \sigma_p n_i e^{(E_i - E_t)/kT}}{\sigma_n[n + n_i e^{(E_t - E_i)/kT}] + \sigma_p[p + n_i e^{(E_i - E_t)/kT}]} \tag{6}$$

and

$$R = \frac{\sigma_p \sigma_n \upsilon_{\text{th}} N_T(np - n_i^2)}{\sigma_n[n + n_i e^{(E_t - E_i)/kT}] + \sigma_p[p + n_i e^{(E_i - E_t)/kT}]} \tag{7}$$

respectively. The term G_{opt} in (2) and (3) is the photogeneration rate and is given by

$$G_{\text{opt}} = \alpha\Phi \cdot \exp(-\alpha y) \tag{8}$$

where Φ is the photon flux, α is the absorption coefficient, and y is the depth from the top surface of the device. The

absorption coefficient is assumed to be 1×10^4 cm^{-1}. Because the ohmic and the gate metals in MESFET's are not transparent to light, it is assumed that no light can penetrate to the regions below the source, the gate, and the drain contacts.

For simplicity, a two-region mobility model is used to describe the field-dependent mobility term for electrons. The two-region model is mathematically expressed as follows:

$$\mu_n = \mu_0, \quad \text{for } E \le \frac{v_s}{\mu_0}$$

$$= \frac{v_s}{E}, \quad \text{for } E \ge \frac{v_s}{\mu_0} \tag{9}$$

where μ_n, μ_0, E, and v_s are the electron mobility, the low-field mobility, the electrical field, and the saturation velocity. The low-field mobility and the saturation velocity for electrons are assumed to be 5000 cm^2/V · s and 1.5×10^7 cm/s, respectively. For holes, the low-field mobility and the saturation velocity are 300 cm^2/V · s and 10^7 cm/s, respectively.

To realistically calculate the gate current across the Schottky contact, the thermionic diffusion current theory and the image-force-induced and dipole-layer-induced barrier lowering effects [21] are applied to the gate boundary condition. The workfunction difference between the Schottky metal and the semiconductor is 0.8 eV. For the source and the drain contacts, the Dirichlet boundary condition is used. For the free surfaces between the source and the gate and between the gate and the drain, the Neumann boundary condition is used.

To solve the coupled equations in (1)–(3), the Gummel method [22] is used. At each bias condition, the convergence criteria are that the drain current change relative to the previous value is less 10^{-5} and at the same time the maximum potential change is less than 10^{-4} kT/q.

IV. Results and Discussions

A. Mechanism for the Increase of Drain Current Due to Illumination

Fig. 2(a) and (b) shows the calculated I_D–V_D characteristics for the device shown in Fig. 1(a) without and with illumination, respectively. The photon flux is 1×10^{20} cm^{-2} · s^{-1} which is typical for a CW double-heterostructure GaAs/AlGaAs laser diode (output power around 2 mW focused to a 50-μm spot) [7]. Comparing Fig. 2(a) with Fig. 2(b), we find a substantial increase of the drain current due to illumination (about 0.6 A/cm). The increase is almost independent of the gate voltage, above threshold. Fig. 3 shows the calculated I_D–V_D characteristics at different photon fluxes. The gate voltage is fixed at 0 V and the fluxes are $\Phi = 0$, 2.5×10^{19}, 5×10^{19}, 7.5×10^{19}, and 1×10^{20} cm^{-2} · s^{-1}. From this figure, it is clear that the drain current increases with the photon flux.

To explain the reason for the increase of drain current due to illumination, the depth profiles for the electron concentration, the hole concentration, and the conduction band edge along the center of the gate at $V_D = 0$ V and $V_G = 0$ V are shown in Fig. 4(a), (b), and (c), respec-

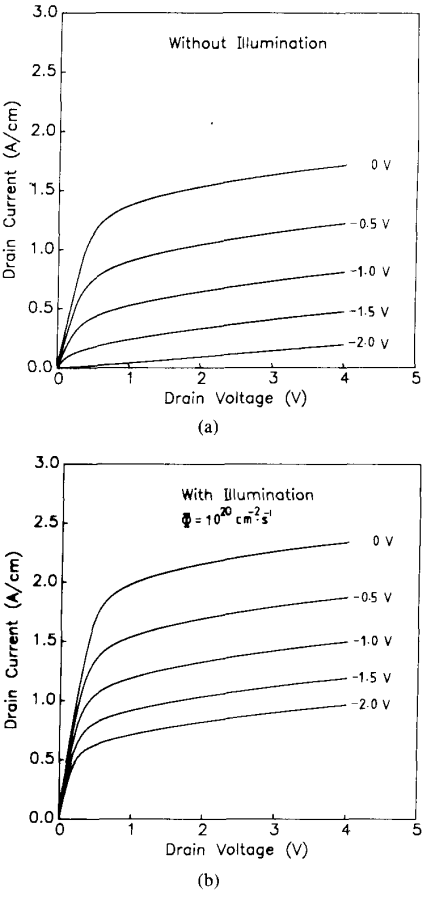

Fig. 2. Calculated I_D–V_D characteristics (a) without and (b) with illumination for the device structure shown in Fig. 1(a). The light flux is 1×10^{20} cm^{-2} · s^{-1}.

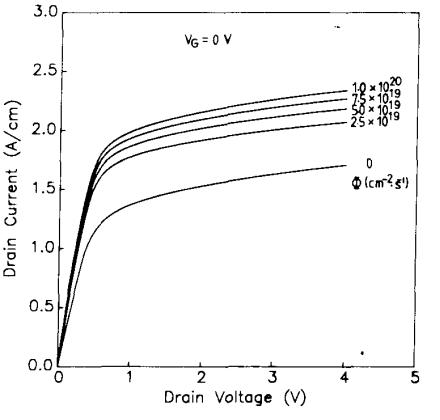

Fig. 3. Calculated I_D–V_D characteristics at different light flux for the device structure shown in Fig. 1(a). $\Phi = 0$, 2.5×10^{19}, 5×10^{19}, 7.5×10^{19}, and 1×10^{20} cm^{-2} · s^{-1}.

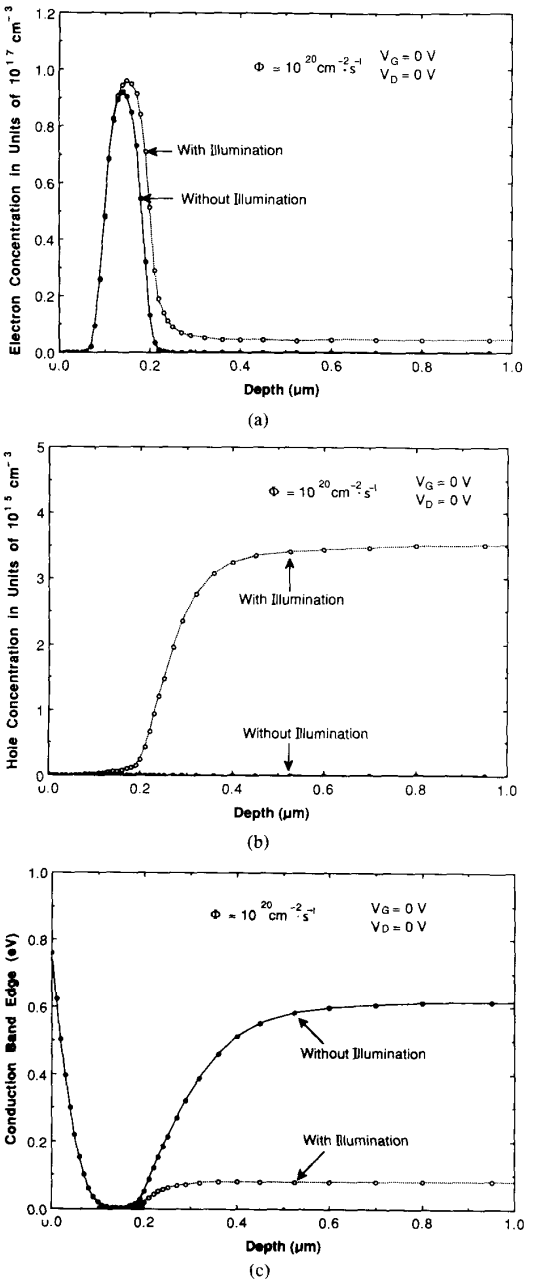

Fig. 4. Depth profiles of (a) the electron concentration, (b) the hole concentration, and (c) the conduction band edge along the center of the gate.

tively. As shown in Fig. 4(c), there is a built-in potential barrier of about 0.6 eV at the channel/substrate interface when there is no light illumination. With illumination, the potential barrier is lowered and the position of the depletion edge on the channel side of the channel/substrate interface moves toward the interface, as shown in Fig. 4(a). The resulting effective channel width, therefore, increases. In the gate depletion region, no significant change of the built-in voltage is observed. The position of the gate depletion edge does not move very much and the concentration of the photogenerated carriers in the depletion junction is far less than the doping concentration in the channel (1×10^{17} cm^{-3}). When the SRH lifetimes for electrons and holes are set to be 1 μs, the magnitude of the drain current is almost the same as that with the lifetimes of 1 ns. So it can be concluded that the gate depletion width and the photogenerated carriers in that region are not responsible for the increase of drain current. The increase of the channel width can be understood from the charge distribution near the channel/substrate interface. Because the electrostatic potential in the substrate side is lower than that in the channel side, the photogenerated electrons and holes, respectively, accumulate on the channel and the substrate sides of the interface under illumination. The charge accumulation can be seen clearly in Fig. 4(b). Because of the charge accumulation, both the depletion region width and the interface potential barrier are reduced. Therefore, the channel width increases and the drain current increases. The phenomena of the interface potential barrier lowering and the accumulation of electrons and holes, respectively, on the channel and the substrate sides are similar to "the photovoltaic effect" of a p-n junction.

Another possible reason for the increase of the drain current is the reduction of the source-to-gate and gate-to-drain resistances in series with the active channel due to illumination. Fig. 5 shows the depth profile of the electron concentration along the center of the region between the source and the gate. It is clear that the effective channel width is larger under illumination than that without illumination. It is expected that the source-to-gate and the gate-to-drain parasitic resistances are reduced due to illumination. However, the peak concentrations in the channel with and without illumination are almost the same, meaning the photoconductivity effect in the n channel is negligible. The reduction of the resistance can be explained by the photovoltaic effect occurring at the channel/substrate interface.

Summarizing these results, the change of gate depletion width and the photogenerated free carriers in the gate depletion junction are negligible and make no significant contribution to the increase of the drain current. The responsible mechanism is the photovoltaic effect occurring at the channel/substrate interface. This conclusion is consistent with the experimental results reported by Edwards [11]. The measured positive voltage across the n channel and the semi-insulating substrate corresponds to the calculated potential barrier lowering at the channel/substrate interface.

B. Reverse Gate Current and Hole Fermi Energy

Another important photoeffect is the measured reverse gate current due to illumination [7], [13]. The calculated gate current versus gate voltage under different photon flux is shown in Fig. 6. The source and the drain voltages are fixed at 0 V. It is found that the reverse gate current is

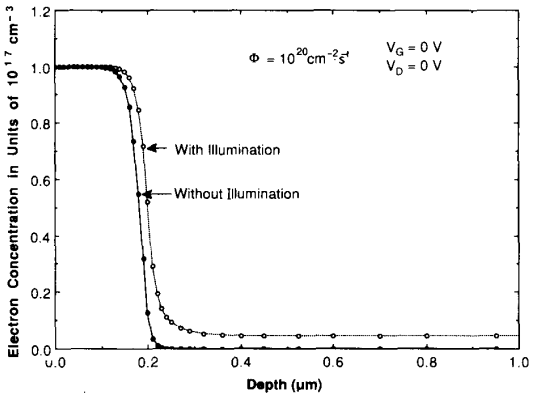

Fig. 5. Depth profiles of the free electron concentration along the center of source-to-gate region with and without illumination.

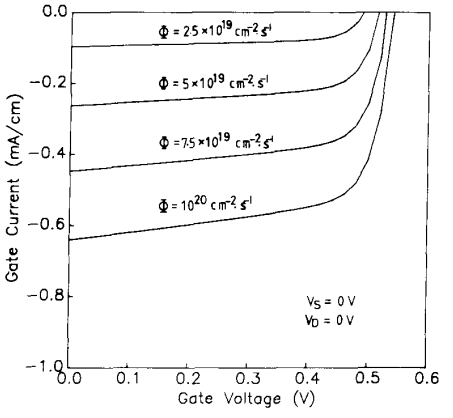

Fig. 6. Calculated I_G–V_G characteristics with the light flux ranged from 2.5×10^{19} to 1×10^{20} cm$^{-2} \cdot$ s^{-1}. The source and the drain voltages are fixed at a voltage of 0 V.

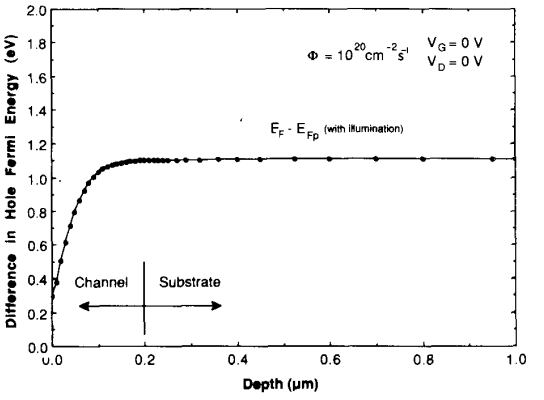

Fig. 7. Depth profile of the difference in the hole Fermi energies with and without illumination.

approximately proportional to the photon flux. Higher open-circuit photovoltage, i.e., the gate voltage at which the gate current falls to zero, is also observed at higher photon flux. For the photon flux ranging from 2.5×10^{19} to 1×10^{20} cm$^{-2} \cdot$ s^{-1}, the open-circuit photovoltage is around 0.5 V. In Salles's measurement [7], for a photon flux around 10^{20} cm$^{-2} \cdot$ s^{-1}, the open-circuit photovoltage is around 0.4 V, which is 0.1 V lower than our calculated value. The 0.1-V difference is probably due to a larger workfunction difference used in this study.

In the past, the difference between the hole Fermi energies with and without illumination (i.e., $E_F - E_{F_p}$) in the gate depletion region has been considered to be equal to the change of the gate built-in voltage [10] and regarded as an important parameter to model the I_D–V_D characteristics [12], [13]. To see the relationship between the difference in hole Fermi energies and the built-in voltage change, we show the depth profile for the difference in the hole Fermi energies without and with illumination in Fig. 7. Throughout the region, the hole Fermi level with illumination is lower than that without illumination. The difference increases with depth. It increases sharply in the gate depletion region and reaches a plateau in the region below the channel. From Fig. 4(c), we can see that the built-in voltage change in the gate depletion region is negligible while the difference in the hole Fermi energies shown in Fig. 7 is significant (larger than 0.3 eV). So there is no close relationship between the built-in voltage and the difference in the hole Fermi energies in the gate depletion region.

The holes generated between the source and gate and between the gate and the drain diffuse to the gate depletion region and are swept out of the gate contact due to the high electric field in that region, so the photovoltaic effect cannot occur at the gate depletion junction. The sweep-out effect has been suggested by Sugeta *et al.* for explaining the high-speed photoresponse mechanism of GaAs MESFET's [4]. Both the steep profile of the hole Fermi energy (shown in Fig. 7) and the low concentration of the holes (shown in Fig. 4(b)) in the gate depletion region confirm the sweep-out effect. To accumulate enough holes in the gate depletion region to change the built-in voltage or the depletion width, the light flux has to be much higher than what has been used or what a regular semiconductor laser can deliver.

C. Device with a Light n-Type Buffer Layer

A MESFET structure commonly used in microwave applications is that shown in Fig. 1(b). An undoped or lightly doped buffer layer (usually n-type) is grown on the substrate prior to the growth of the channel layer. The thickness of the buffer layer is chosen so that the free carriers in the layer are totally depleted by the substrate to buffer layer interface potential. The simulated I_D–V_D characteristics of such a device at different photon fluxes are shown in Fig. 8. The gate voltage is 0 V and the photon fluxes Φ are 0, 2.5×10^{19}, 5×10^{19}, 7.5×10^{19}, and 1×10^{20} cm$^{-2} \cdot$ s^{-1}. Comparing Fig. 3 with Fig. 8, we see that the drain current for the device with a buffer layer is higher than that without a buffer layer. The increase of the drain current due to light illumination is substantial but is lower than that obtained in the device without a buffer layer. These phenomena are explained by the fact

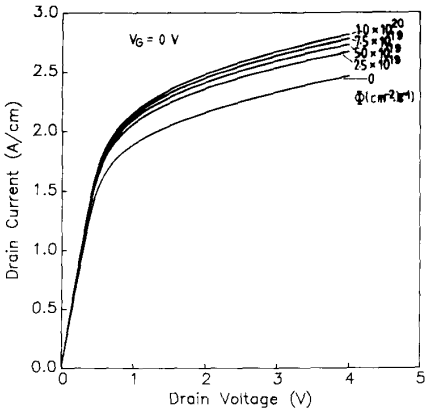

Fig. 8. Calculated I_D-V_D characteristics at different light flux for the device structure shown in Fig. 1(b). Φ = 0, 2.5 × 10^{19}, 5 × 10^{19}, 7.5 × 10^{19}, and 1 × 10^{20} $cm^{-2} \cdot s^{-1}$.

that the depletion width on the channel side due to the forming of the channel/substrate space-charge region and the depletion width change due to the illumination are reduced by the n-type buffer layer. However, the photovoltaic effect is still strong enough to cause a substantial increase in the drain current.

V. Conclusions

The photoeffects on the I-V characteristics of the GaAs MESFET's have been studied by a two-dimensional numerical method. The photovoltaic effect occurring at the channel/substrate interface is found to be the mechanism responsible for the substantial increase of the drain current. The photovoltaic effect causes the lowering of the interface potential barrier and the reduction of the width of the space-charge region in the channel side, widening effective channel thickness. The reverse gate current is caused by the sweep-out effect which results in a large gradient in the depth profile of the hole Fermi energy in the gate depletion region. For devices with an n-type buffer layer, the increase of the drain current due to illumination is less than that for devices without a buffer layer, due to a smaller change of the depletion width. However, the increase of the drain current is still substantial.

References

[1] C. Baack, G. Elze, and G. Walf, "GaAs M.E.S.F.E.T.: A high-speed optical detector," *Electron. Lett.*, vol. 13, no. 7, p. 193, 1977.
[2] J. Pan, "GaAs MESFET for high speed optical detection," in *SPIE Int. Tech. Symp.* (San Diego, CA), 1978.
[3] J. M. Osterwalder and B. J. Rickett, "GaAs MESFET demodulates gigabit signal rates from GaAlAs injection laser," *Proc. IEEE*, vol. 67, no. 6, pp. 966-968, June 1979.
[4] T. Sugeta and Y. Mizushima, "High speed photoresponse mechanism of a GaAs-MESFET," *Japan. J. Appl. Phys.*, vol. 19, no. pp. L27-29, Jan. 1980.
[5] H. J. Sun, R. J. Gutmann, and J. M. Borrego, "Photoeffects in common-source and common-drain microwave GaAs MESFET oscillators," *Solid-State Electron.*, vol. 24, no. 10, pp. 935-940, 1981.
[6] H. Mizuno, "Microwave characteristics of an optically controlled GaAs MESFET," *IEEE Trans. Microwave Theory Tech.*, vol. MTT-31, no. 7, pp. 596-600, July 1983.
[7] A. A. Salles, "Optical control of GaAs MESFET's," *IEEE Trans. Microwave Theory Tech.*, vol. MTT-31, no. 10, pp. 812-820, Oct. 1983.
[8] R. N. Simons, "Microwave performance of an optically controlled AlGaAs/GaAs high electron mobility transistor and GaAs MESFET," *IEEE Trans. Microwave Theory Tech.*, vol. MTT-35, no. 12, pp. 1444-1455, Dec. 1987.
[9] A. J. Seeds and A. A. Salles, "Optical control of microwave semiconductor devices," *IEEE Trans. Microwave Theory Tech.*, vol. 38, no. 5, pp. 577-585, May 1990.
[10] J. Graffeuil, P. Rossel, and H. Martinot, "Light-induced effects in GaAs F.E.T.s," *Electron. Lett.*, vol. 15, no. 14, pp. 439-441, July 1979.
[11] W. D. Edwards, "Two and three terminal gallium arsenide FET optical detectors," *IEEE Electron Device Lett.*, vol. EDL-1, no. 8, pp. 149-150, Aug. 1980.
[12] R. N. Simons and K. B. Bhasin, "Analysis of optically controlled microwave/millimeter-wave device structures," *IEEE Trans. Microwave Theory Tech.*, vol. MTT-34, no. 12, pp. 1349-1355, Dec. 1986.
[13] J. L. Gautier, D. Pasquet, and P. Pouvil, "Optical effects on the static and dynamic characteristics of a GaAs MESFET," *IEEE Trans. Microwave Theory Tech.*, vol. MTT-33, no. 9, pp. 819-822, 1985.
[14] S. Mishra, V. K. Singh, and B. B. Pal, "Effect of radiation and surface recombination on the characteristics of an ion-implanted GaAs MESFET," *IEEE Trans. Electron Devices*, vol. 37, no. 1, pp. 2-10, Jan. 1990.
[15] S. N. Mohammad, M. S. Unlu, and H. Morkoç, "Optically controlled current-voltage characteristics of ion-implanted MESFETs," *Solid-State Electron.*, vol. 33, no. 12, pp. 1499-1509, 1990.
[16] C. Kocot and C. A. Stolte, "Backgating in GaAs MESFET's," *IEEE Trans. Electron Devices*, vol. ED-29, no. 7, pp. 1059-1064, July 1982.
[17] H. C. Casey Jr., D. D. Sell, and K. W. Wecht, "Concentration dependence of the absorption coefficient for n-type and p-type GaAs between 1.3 and 1.6 eV," *J. Appl. Phys.*, vol. 46, no. 1, pp. 250-257, Jan. 1975.
[18] G. Baccarani, M. Rudan, R. Guerrieri, and P. Ciampolini, "Physical models for numerical device simulations," in *Process and Device Modeling*, W. L. Eng, Ed. Amsterdam, The Netherlands: North-Holland, 1986, pp. 107-158.
[19] H. C. Casey Jr., B. I. Miller, and E. Pinkas, "Variation of minority-carrier diffusion length with carrier concentration in GaAs liquid-phase epitaxial layers," *J. Appl. Phys.*, vol. 44, pp. 1281-1287, Mar. 1973.
[20] G. M. Martin, "Key electrical parameters in semi-insulating materials: The methods to determine them in GaAs," *Inst. Phys. Conf. Ser.*, pp. 13-28, 1980.
[21] S. M. Sze, *Physics of Semiconductor Devices*. New York: Wiley, 1981.
[22] H. K. Gummel, "A self-consistent iterative scheme for one-dimensional steady state transistor calculations," *IEEE Trans. Electron Devices*, vol. ED-11, pp. 455-465, 1964.

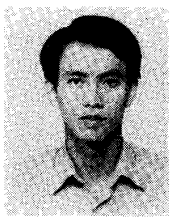

Shih-Hsien Lo (S'90) was born in Taiwan, Republic of China, in 1964. He received the B.S. degree in electrical engineering from National Cheng-Kung University in 1986 and the M.S. and Ph.D. degrees in electronics engineering from National Chiao-Tung University in 1988 and 1991, respectively. Currently he is doing two years' military service.

His research interests are in the areas of numerical modeling and electrical characterization of GaAs MESFET devices.

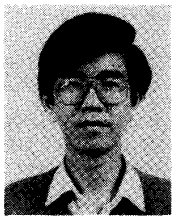

Chien-Ping Lee (M'80) received the B.S. degree in physics from National Taiwan University in 1971 and the Ph.D. degree in applied physics from California Institute of Technology, Pasadena, in 1978. While at Caltech, he worked on GaAs-based integrated optics. He was credited with the design and fabrication of several important optoelectronic components, including the first integrated optoelectronic circuit, which consists of a laser and a Gunn device fabricated on a same substrate.

After graduation, he joined Bell Laboratories, where he worked on integrated optics and semiconductor lasers. He joined Rockwell International in 1979 and worked on GaAs integrated circuits. He did extensive work on substrate-related effects such as the orientation effect and the backgating effect. In 1982 he was promoted to be a project leader and later a manager with responsibility for the development of ultra-high-speed integrated circuits using high electron mobility transistors. He received the Engineer of the Year award in 1982 for his contribution in GaAs IC and HEMT technologies. In 1987 he joined National Chiao Tung University, where he was a Professor and the Director of the Semiconductor Research Center. He was also the director of the National Submicron Device Laboratory in charge of the construction of the first sub-micrometer device research center in the country. He returned to Rockwell as the manager of the Advanced Devices Department in 1990, responsible for the development of advanced III-V devices. In 1992, he returned to National Chiao Tung University as a professor. His current research interests are in the areas of III-V optoelectronic devices, MBE technology, heterostructure devices and physics, and device simulation.